Z_e and ρ_e – A Different Dual-energy X-Ray CT Feature Space

CIRMS, NIST, Gaithersburg, Maryland

April 27–29, 2015

Harry E. Martz, Jr., Steve Azevedo, Bill Brown, Kyle Champley, Jeff Kallman, Dan Schneberk, Isaac Seetho, Jerel Smith, Maurice Aufderheide

Lawrence Livermore National Laboratory

Nondestructive Characterization Institute

finalized on
April 20, 2015
Version 7

LLNL-PRES-669952

This work was performed under the auspices of the U.S. Department of Energy by Lawrence Livermore National Laboratory under Contract DE-AC52-07NA27344. Lawrence Livermore National Security, LLC

Summary and Future Work

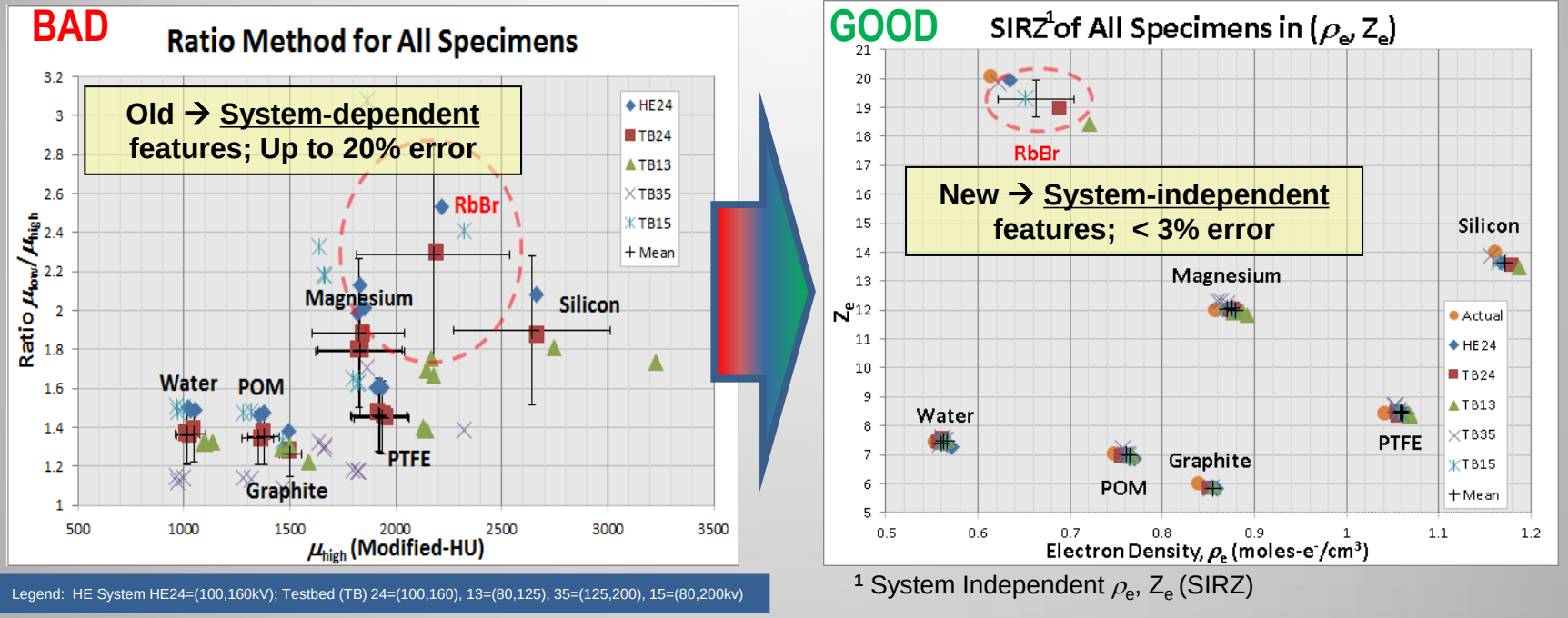

Legend: HE System HE24=(100,160kV); Testbed (TB) 24=(100,160), 13=(80,125), 35=(125,200), 15=(80,200kv)

[1] System Independent ρ_e, Z_e (SIRZ)

- **New X-ray features (ρ_e,Z_e) gave same results on two different MicroCT systems at LLNL; they are system-independent[2]**
  - Tested with 5 bare (homogeneous), 2 complex (heterogeneous) and 1 high-Z specimens
  - Used 2 different MicroCT scanners, 2 different detectors and 5 different spectra
  - No beam-hardening compensation (BHC) needed
  - Achieved <3% accuracy and <2% precision (req't ±3%) across all system variations (vs ±20% with current method) without RbBr
- **Future Work**
  - Automate and employ (ρ_e,Z_e) features for dual-energy CT systems at LLNL
  - Show that (ρ_e,Z_e) feature space
    - Can translate across different labs' MicroCTs and to other CT systems
    - Is backward compatible; i.e., we can use the data already acquired
  - Replace (μ_H, μ_L / μ_H) features with (ρ_e,Z_e)

[2] Azevedo, S. G., System-Independent Dual-energy Computed Tomography for Characterization of Materials, IEEE TRANSACTIONS ON NUCLEAR SCIENCE, VOL. *, NO. *, MONTH 2015

Objectives and Requirements

- **Objective of this R&D task**
  - **Find a "system-independent" x-ray feature space suitable for characterizing materials for DOE, DoD, DHS, etc.**
    - **Used for quality assurance and certification of materials and assemblies**

- **Requirements**
  - **Shall produce features with accuracy and precision to less than 3% of "ground truth" (known physical properties) across two different LLNL MCT systems**
  - **Shall be based on dual-energy X-ray CT, employing pairs of spectra ranging from 80 to 200 kV (Note: typical MCT and EDS systems are 100 to 180 kV)**
  - **Shall be backward compatible; *i.e.*, able to be applied to historical data; we cannot afford to re-acquire previously acquired data**

What causes X-ray attenuation by materials?

- X-ray attenuation at the energy levels below 1.022 MeV is largely due to two sources:
  - Photoelectric effect: X-rays are completely absorbed by electrons in the specimen, ejecting the electron.
  - Compton scatter: X-rays are deflected by electrons with low binding energy, ejecting the electron and scattering the x-ray.
- X-ray attenuation coefficients can be decomposed into a linear combination of photoelectric and Compton contributions (conventional approximation)
- Full attenuation information over a broad range of energy values can be represented using a set of energy-dependent basis functions

Photoelectric absorption

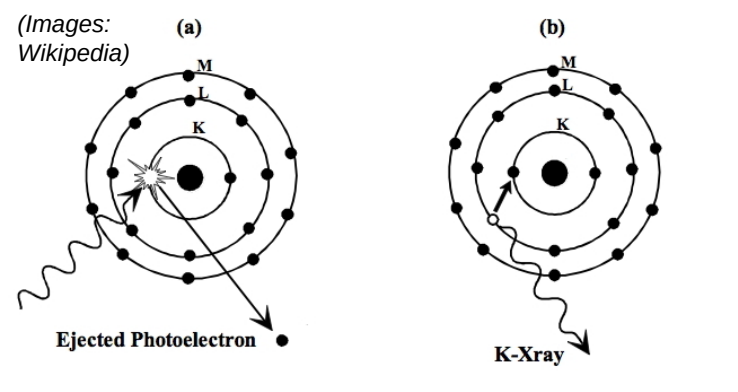

Compton scattering

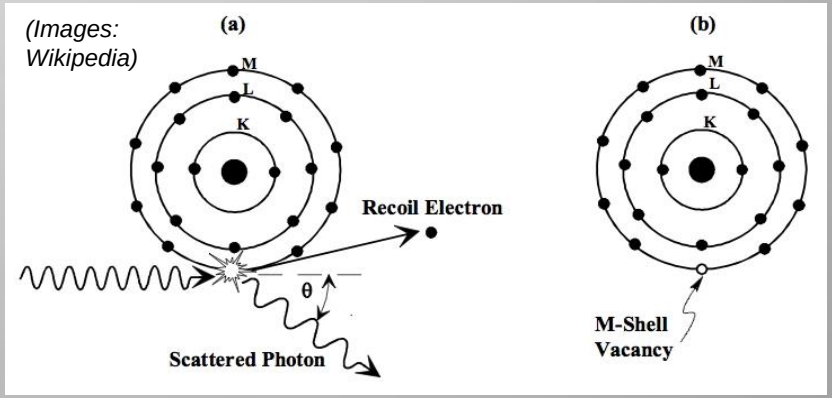

R. E. Alvarez, A. Macovski, *Energy-selective Reconstructions in X-ray Computerized Tomography*, Phys. Med. Biol., 1976, vol. 21, no. 5, 733-744.

X-ray Signatures / Feature Space and Definitions

Physical properties:

- **Z – Atomic number of an elemental material**
- **ρ – Physical density (g/cm^3); mean over volume of a specimen**

X-ray properties: (all depend also on the X-ray energy)

- **μ_{low} – Linear attenuation coefficient (mm^{-1}) for a low-energy spectrum [Needs BHC using a reference material (Al or water)]**
- **μ_{high} – Linear attenuation coefficient (mm^{-1}) for a high-energy spectrum**
- **Z_{eff} – Effective Z of a composite using Wikipedia method**
- **$^{L}Z_{eff}$ – Effective Z derived from a curve relating Z_{eff}s for reference materials and the ratio of μ_{low} / μ_{high}, where μ_{low} is reconstructed using aluminum-reference-based BHC**
- **$^{LW}Z_{eff}$ – Same, except using water-reference-based BHC for μ_{low}**
- **Z_e – Effective atomic number of a material defined by Ze paper***
- **ρ_e – Electron density (e-mol/cm^3); X-rays respond to ρ_e**

---

* Smith, JA, Kallman, J, and Martz, H, "Case for an Improved Effective-Atomic-Number for the Electronic Baggage Scanning Program." LLNL-TR-520312-REV-1, October 16, 2012.

X-ray Signatures / Feature Space and Definitions

Physical properties:

- **Z – Atomic number of an elemental material**
- **ρ – Physical density (g/cm^3); mean over volume of a specimen**

X-ray properties: (all depend also on the X-ray energy)

- **μ_{low} – Linear attenuation coefficient (mm^{-1}) for a low-energy spectrum [Needs BHC using a reference material (Al or water)]**
- **μ_{high} – Linear attenuation coefficient (mm^{-1}) for a high-energy spectrum**
- **Z_{eff} – Effective Z of a composite using Wikipedia method**
- **$^{L}Z_{eff}$ – Effective Z derived from a curve relating Z_{eff}s for reference materials and the ratio of μ_{low} / μ_{high}, where μ_{low} is reconstructed using aluminum-reference-based BHC**
- **$^{LW}Z_{eff}$ – Same, except using water-reference-based BHC for μ_{low}**
- **Z_e – Effective atomic number of a material defined by Ze paper*** New
- **ρ_e – Electron density (e-mol/cm^3); X-rays respond to ρ_e** Seldom used

Increasing System Independence

* Smith, JA, Kallman, J, and Martz, H, "Case for an Improved Effective-Atomic-Number for the Electronic Baggage Scanning Program." LLNL-TR-520312-REV-1, October 16, 2012.

What are Z_e, ρ_e?

- Z_e is an alternative definition of effective atomic number of a material developed at LLNL, and based on material x-ray cross sections.
  - X-ray cross sections relate the degree of attenuation and scattering of incident x-rays by a material
  - Tool developed at LLNL, ZeCalc.
  - Input is a set of spectral endpoint energies and material composition.
- ρ_e is the electron density, defined for a single element material as: $\rho_e = \frac{\rho Z}{A}$
  - ρ is material mass density.
  - Z is atomic number.
  - A is atomic mass.
- Experimental results show a (Z_e, ρ_e) representation to have better resolution of different materials than methods using the high and low energy reconstructions.
- In addition, materials with identical Z_e are shown to have closer x-ray cross section than materials with identical Z_{eff}.

CALCULATIONS OF Z_E AND Z_{EFF} FOR SELECTED MATERIALS

Material[a]	Formula	ρ g/cm^3	ρ_e [b]	Z_e @ 100kV	Z_e @ 160kV	Z_{eff} p=3.8
Lexan	$C_{15}H_{16}O_2$	1.21	0.647	6.12	6.07	6.19
POM	$(CH_2O)_n$	1.42	0.754	7.01	6.97	7.07
Water	H_2O	1.00	0.554	7.44	7.39	7.54
PTFE	$(C_2F_4)_n$	2.20	1.056	8.43	8.43	8.50
Silica	SiO_2	2.65	1.323	11.64	11.62	11.85
PVC	$(C_2H_3Cl)_n$	1.35	0.691	14.07	14.06	14.44
12% LiBr	$LiBr/H_2O$	1.05	0.565	16.43	16.57	**18.68**
19% RbBr	$RbBr/H_2O$	1.17	0.623	19.95	20.08	**22.18**

[a] The lithium bromide and rubidium bromide materials (bottom two rows) are aqueous solutions with percentage by weight.

Four General Methodologies Considered

- **Four general methodologies have been used**
  - **Ratio μ_L/μ_H vs μ_H (LLNL) in Livermore-Modified Hounsfield Units (LMHU*) (LLNL)**
  - **$^{L}Z_{eff}$ vs μ_H**
  - **Photoelectric-Compton Decomposition**
    - **Alvarez & Macovsky, 1976**
    - **Ying, Naidu, Crawford (YNC), 2006**
    - **System-Independent Rho-e/Ze (SIRZ) at LLNL, 2014**
  - **Direct Decomposition (still under development)**

* Where LLNL modified Hounsfield units with respect to water. To obtain the LAC in LMHU for some material at any energy, we multiply by 1000 and divide by the LAC of water at an X-ray energy of 160 kV with aluminum and copper filters.

Four General Methodologies Considered
Three of these methods were evaluated

- **Four general methodologies have been used**
  - **Ratio μ_L/μ_H vs μ_H (LLNL) in Livermore-Modified Hounsfield Units (LMHU*) (LLNL)**
  - **${}^{L}Z_{eff}$ vs μ_H**
  - **Photoelectric-Compton Decomposition**
    - **Alvarez & Macovsky, 1976**
    - **Ying, Naidu, Crawford (YNC), 2006**
    - **System-Independent Rho-e/Ze (SIRZ) at LLNL, 2014**
  - **Direct Decomposition (still under development)**

* Where LLNL modified Hounsfield units with respect to water. To obtain the LAC in LMHU for some material at any energy, we multiply by 1000 and divide by the LAC of water at an X-ray energy of 160 kV with aluminum and copper filters.

System-Independent ρ_e/Z_e (SIRZ) Method

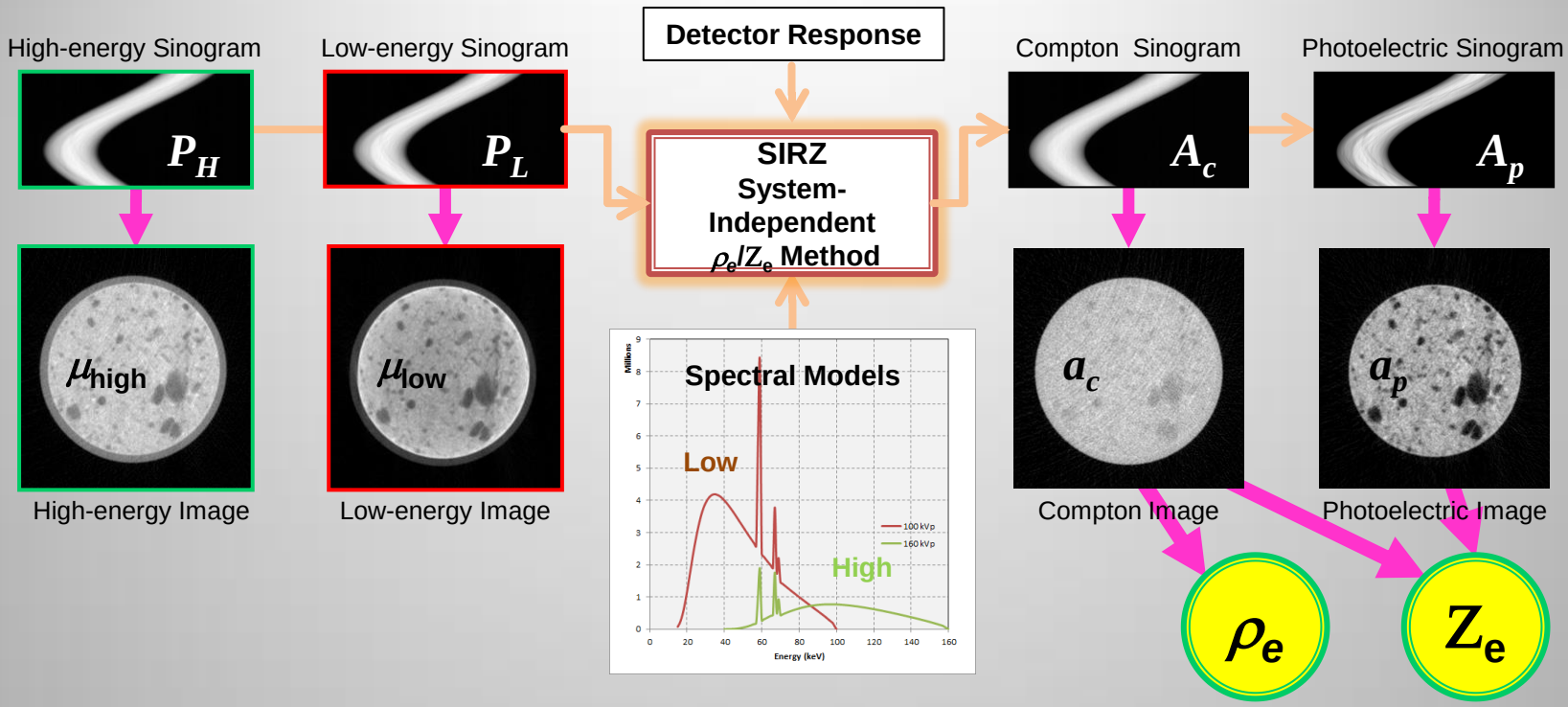

- **High- and low-energy sinograms are decomposed into Compton and Photoelectric contributions using X-ray spectral response (source/detector) models**
- **These sinograms are reconstructed into Compton (a_c) and Photoelectric (a_p) images**
- **Mean values inside the specimen are calculated: $\bar{a}_c$ and $\bar{a}_p$**
- **Then, $\rho_e = K(\bar{a}_c)$ and $Z_e = k(\bar{a}_p/\bar{a}_c)^{1/n}$**
  - **where K, k and n are empirically determined constants obtained through a calibration procedure using the Reference Standards**

Note that beam-hardening compensation (BHC) is not needed.

MicroCTs characterize specimens at 150-µm voxels

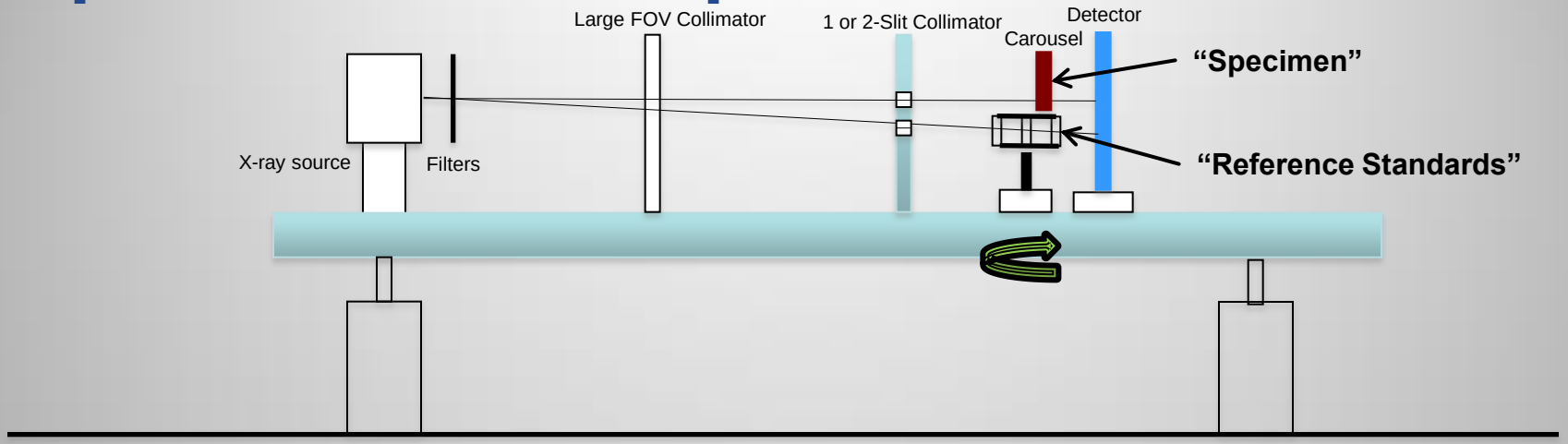

X-Ray Source
- Brehmstrahlung Source
- End point potential up to 450 kV
- (200 kV max. for this study)

Filters
- Used to filter beam spectra
- Typical filters used Cu and/or Al

Large FOV Collimator
- Collimates the X-ray cone beam
- Removes primary beam outside detector
- Reduces scatter

1 or 2-Slit Collimator
- 1 is for lower 2-mm slit
  - Upper collimator is removed for larger images of the specimen
- 2 is for two 2-mm slits
  - Reduces primary beam
  - Reduces Scatter

Carousel
- Houses the HME sample on top
- Houses Reference Standards below
- Attached to rotation stage for CT data acquisition

Detector
- Amorphous silicon flat panel
- Converts X-rays to digital image
- Outputs the image to disk

If the system spectral response (source/detector) changes, then (μ_{high}, μ_{low}/μ_{high}) also changes, while (Z_e, ρ_e) space does not change if spectral response change is quantified.

Reference Standards

- Reference materials were acquired and characterized at LLNL
  - High confidence in material composition (POM is is Acetyl co-polymer, similar to Delrin, PTFE is Teflon)
  - More accurate Z_e, ρ_e values for confidence in results
  - References selected to expand the range in Z relative to current specimens/materials to be characterized

REFERENCE MATERIALS USED IN THE DECT EXPERIMENTS

Reference Material	Chemical Makeup	Bulk Density, ρ (g/cc)	Electron Density[b], ρ_e (moles-e$^-$/cm^3)	Effective Atomic Number[b], Z_e
Graphite	C	1.804 ± 0.02	0.901 ± 0.003	6.00 ± 0.01
POM	$(CH_2O)_n$	1.403 ± 0.02	0.748 ± 0.003	7.01 ± 0.01
Water[a]	H_2O	0.998 ± 0.02	0.554 ± 0.002	7.43 ± 0.01
PTFE	$(C_2F_4)_n$	2.175 ± 0.02	1.044 ± 0.003	8.44 ± 0.01
Magnesium	Mg	1.736 ± 0.02	0.857 ± 0.003	12.00 ± 0.01
Silicon	Si	2.331 ± 0.02	1.162 ± 0.003	14.00 ± 0.01

[a] De-ionized reagent-grade water (from Fisher Scientific, Cat # 23-751-610) was contained in a polyethylene bottle.

[b] Z_e and ρ_e values were supplied by ZeCalc [32] using a 160 keV spectrum and a nominal areal density of 2.5 g/cm^2.

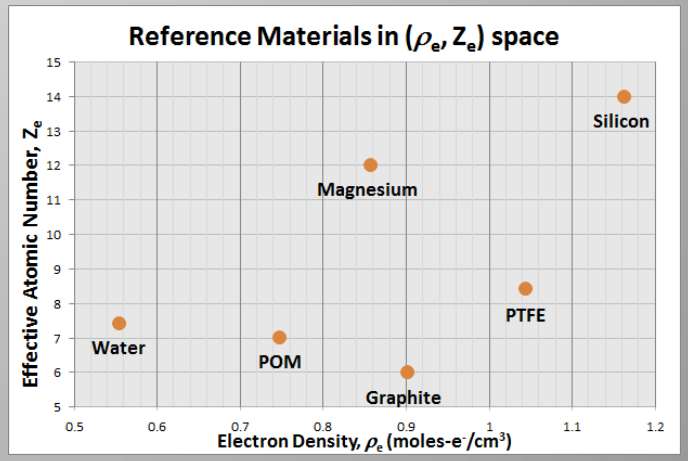

Specimens

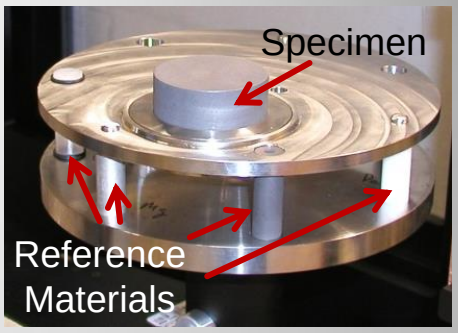

MicroCT Carousel

Three types of specimens were used to test system performance

- Homogeneous Specimens correspond to reference materials from graphite, Z=6, to silicon, Z=14 (5 specimens)
- Heterogeneous Specimens (at right) to examine behavior with mixed materials (2 specimens)
- High-Z Specimen of Rubidium Bromide (RbBr) solution (Z=20) to test the techniques in cases where the specimen is well out of the reference-material range (1 specimen)

HOMOGENEOUS SPECIMENS USED IN THE DECT EXPERIMENTS

Specimen	Diam. (mm)	Bulk Density, ρ (g/cc)	Electron Density[b], ρ_e (moles-e$^-$/cm^3)	Effective Atomic Number[b], Z_e
Graphite	50.9	1.682 ± 0.002	0.901 ± 0.003	6.00 ± 0.01
Water[a]	36.9 id 38.9 od	0.998 ± 0.002	0.554 ± 0.002	7.43 ± 0.01
PTFE	55.3	2.173 ± 0.002	1.042 ± 0.003	8.44 ± 0.01
Magnesium	25.3	1.738 ± 0.002	0.858 ± 0.003	12.00 ± 0.01
Silicon	25.3	2.329 ± 0.002	1.161 ± 0.003	14.00 ± 0.01

[a] The water was contained in a high-density polyethylene bottle with inner and outer diameters listed; density and Z_e numbers are for water alone.
[b] Z_e and ρ_e values were supplied by ZeCalc [32] using a 160 keV spectrum and a nominal areal density of 2.5 g/cm^2.

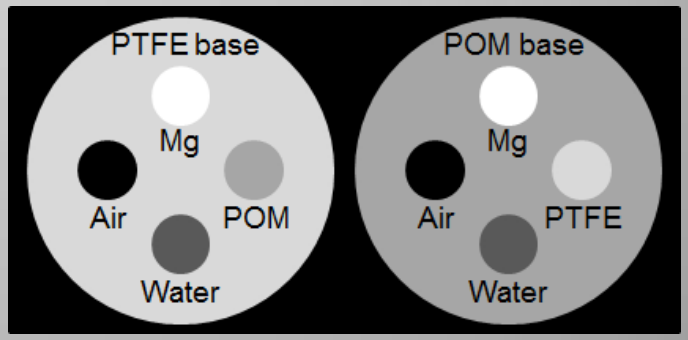

Heterogeneous Specimens

MicroCT Systems and Spectra

- Two different MicroCT systems, with different detectors, were used
  - HE – In the High-explosives Application Facility had a **Thales** panel (2 spectra)
  - TB – In the NCI Test Bed had a **Perkin Elmer** panel (5 spectra)
- Spectra were selected to cover a broad range of endpoint energy values, and to connect to current practice (using 100kV, 160kV)

MICRO-CT SCANNERS, SPECTRA AND FILTERS USED IN EXPERIMENTS

		Endpoint Energy (keV)[a]				
Micro-CT Scanner	**Filter**	**80**	**100**	**125**	**160**	**200**
HE filter thickness (in mm) →	Aluminum		1.94		1.94	
	Copper		0		1.91	
TB filter thickness (in mm) →	Aluminum	0.41	1.96	0	1.96	0
	Copper	0	0	0.92	1.85	2.87
	Steel	0.13	0	0	0	0
Spectrum Number		**1**	**2**	**3**	**4**	**5**

[a] The shaded boxes indicate the scans that were not performed.

Experiments and Data Analysis

- Experimental Micro-CT scans were conducted to evaluate the system-independence of X-ray feature spaces. SOPs for were followed: system alignment, source quality checks, detector calibration, background and dark-current measurement, and acquisition of specimen and reference-material sinograms (720 projs over 360^{o})
- All three types of specimens of different sizes were scanned on the two Micro-CT systems (HE and TB) using multiple energy spectra
  - On TB, all specimens were scanned and CT data were acquired using all five spectra
  - On HE, due to scanner availability, only two spectra (100 keV and 160 keV) were acquired
- Reference specimens were scanned simultaneously on the lower carousel
- Pairs of scans were processed as dual-energy CT data using
  - Ratio – μ_L/μ_H vs μ_H (LLNL)
  - YNC – Z_{eff} vs μ_H (as obtained using LLNL PCD)
  - SIRZ – Z_e vs ρ_e (as obtained using LLNL PCD)
- Calculated mean and standard deviation as a measure of uncertainty
  - Precision – Standard deviation / mean
  - Accuracy – |(Mean – GT) / GT| [for SIRZ only because the ground truth (GT) of μ is not known)

Representative MicroCT images

Upper slit CT slice

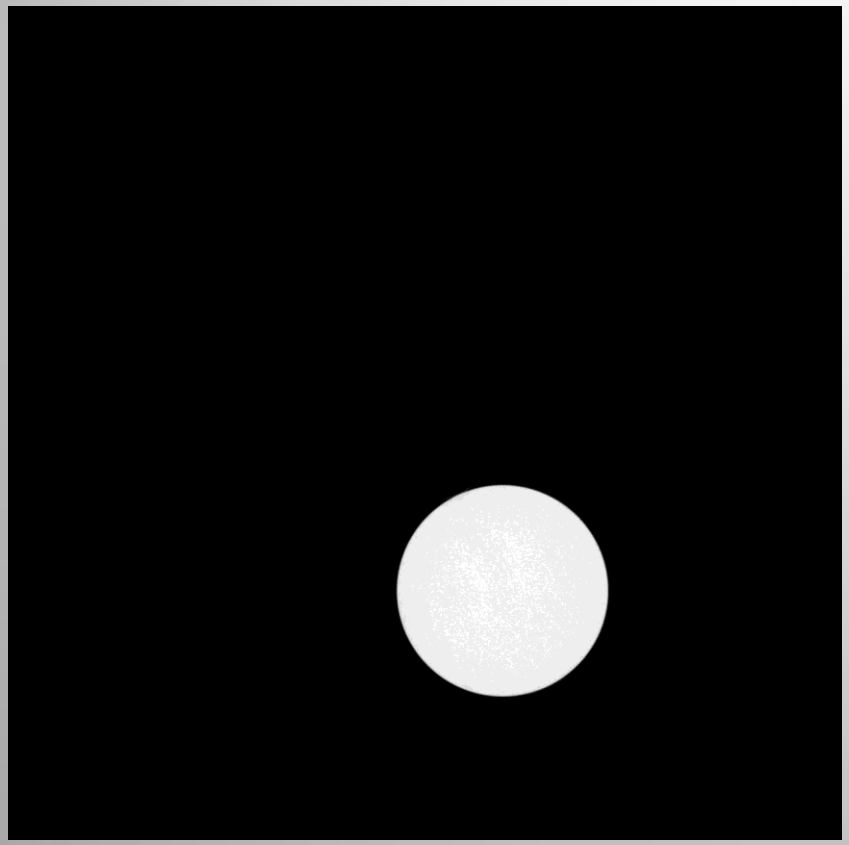

2-in. graphite specimen in 100kV TB MicroCT

Lower slit CT slice

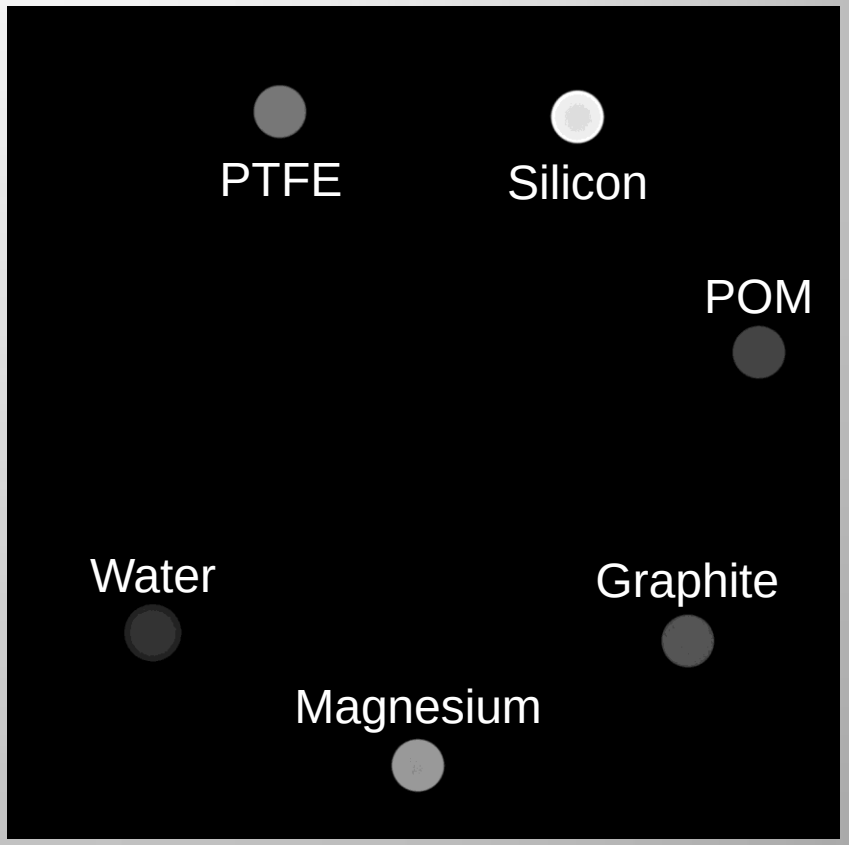

Reference Materials in 100kV TB MicroCT

Initial Efforts: Ratio, μ_L/μ_H, vs High Energy, μ_H

- Initial efforts at LLNL made comparisons between the high energy channel attenuation (μ_H) and the ratio of attenuation at two energies
  - High energy channel approximately trends with density of the material
  - Ratio between the two energies approximately trends with effective atomic number.

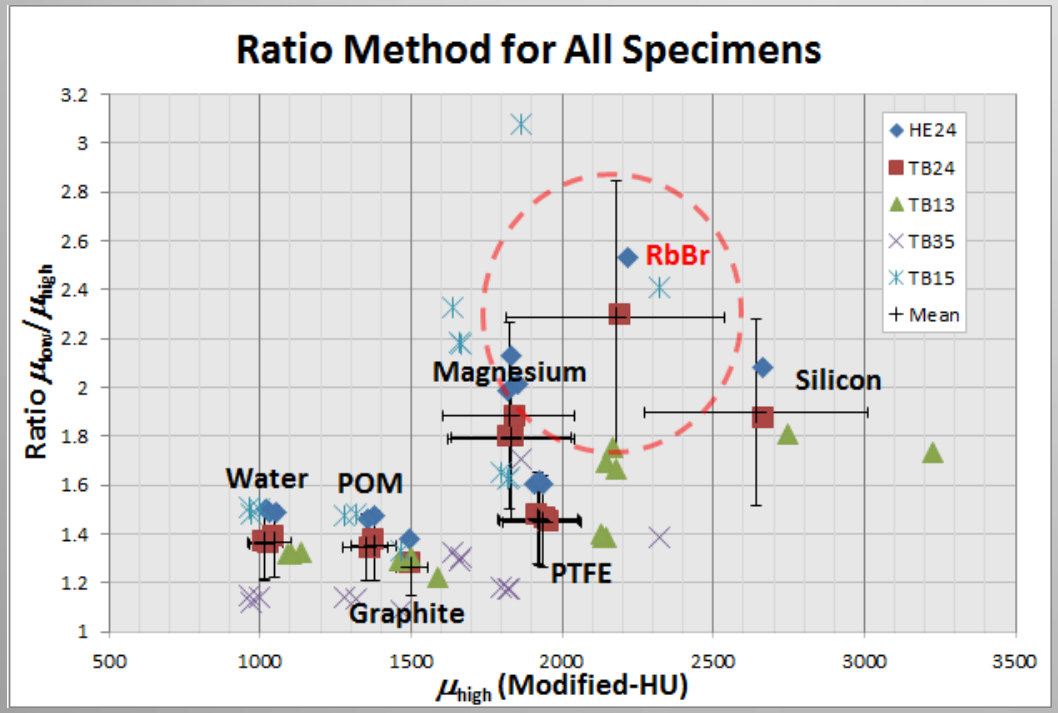

- Problems:
  - High- and low-energy attenuation values vary across systems, spectra and samples
  - High-low attenuation ratio is a function of thickness of materials
  - Difficult to compare materials between machines

YNC:
Z_{eff} vs High Energy, μ_H

- Produces improvement in Zeff precision over the Ratio method

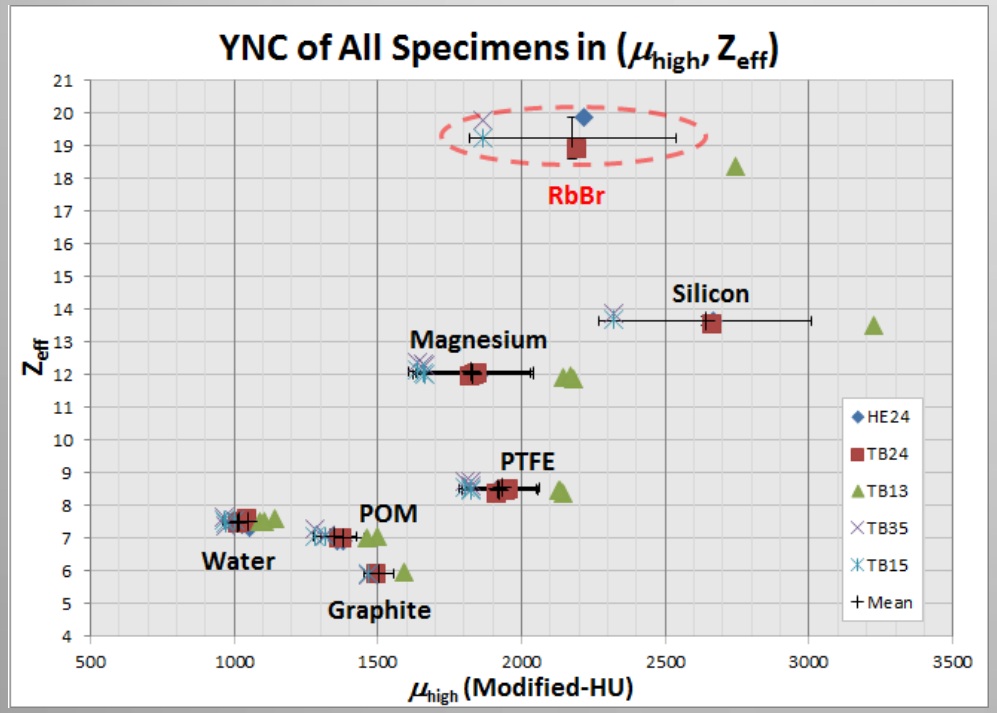

- Problems:
  - The use of μ_H is still problematic for comparing systems and spectra
  - Difficult to compare materials between machines

SIRZ: Z_e vs ρ_e

- Accuracy and precision of SIRZ is much improved

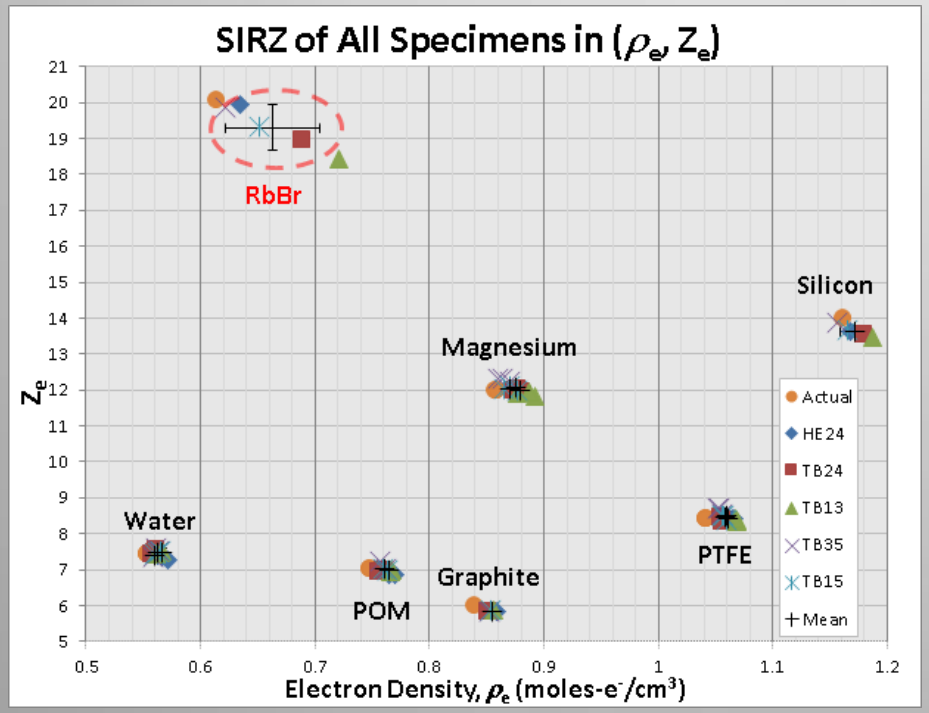

- Problems:
  - For the high-Z specimen (RbBr), both precision and accuracy suffer because it is out of the range of the reference materials
    - A wider range of reference materials could improve these high-Z results

Results – Precision and Accuracy

- Tables show Precision (left) for the specimens and Accuracy (right, for SIRZ only) for several spectra with and without RbBr
  - Low- and high-energy attenuation values (μ_L, μ_H) are computed using beam hardening compensation based on water
  - Z_e, ρ_e show much better precision (<2%, <1%) than ratio (<20%) or μ_H (<14%)

Precision

STANDARD DEVIATION (IN %) FOR THE SPECIMENS

Precision (%) For Specimen[a]	Ratio	YNC μ_{high}	SIRZ ρ_e	YNC Z_{eff}	SIRZ Z_e
Graphite	8.9	3.4	0.4	0.4	0.4
POM	10.3	5.4	0.6	1.4	1.4
Water	10.9	5.3	0.5	0.8	0.8
PTFE	12.8	6.8	0.6	1.3	1.3
Magnesium	19.2	11.4	0.9	1.3	1.3
Silicon	20.0	14.0	1.0	1.1	1.1
19% RbBr	24.5	16.5	6.2	3.3	3.3

[a] The water, magnesium, POM and PTFE estimates include results from the relevant homogeneous regions in the heterogeneous specimens.

Accuracy

AVERAGE ABSOLUTE ERROR (%) OF YNC AND SIRZ ESTIMATES

Accuracy (%)	With RbBr		Without RbBr	
	All spectra	100/160[a]	All spectra	100/160[a]
Z_e, Z_{eff} Mean	0.87	0.98	0.69	0.84
Z_e, Z_{eff} Max	3.73	2.95	2.57	2.93
ρ_e Mean	1.80	1.85	1.66	1.75
ρ_e Max	8.02	7.69	2.43	2.47

[a] The "100/160" column lists accuracy for the 100- and 160-keV spectra only, which are in common between scanners.

Summary and Future Work

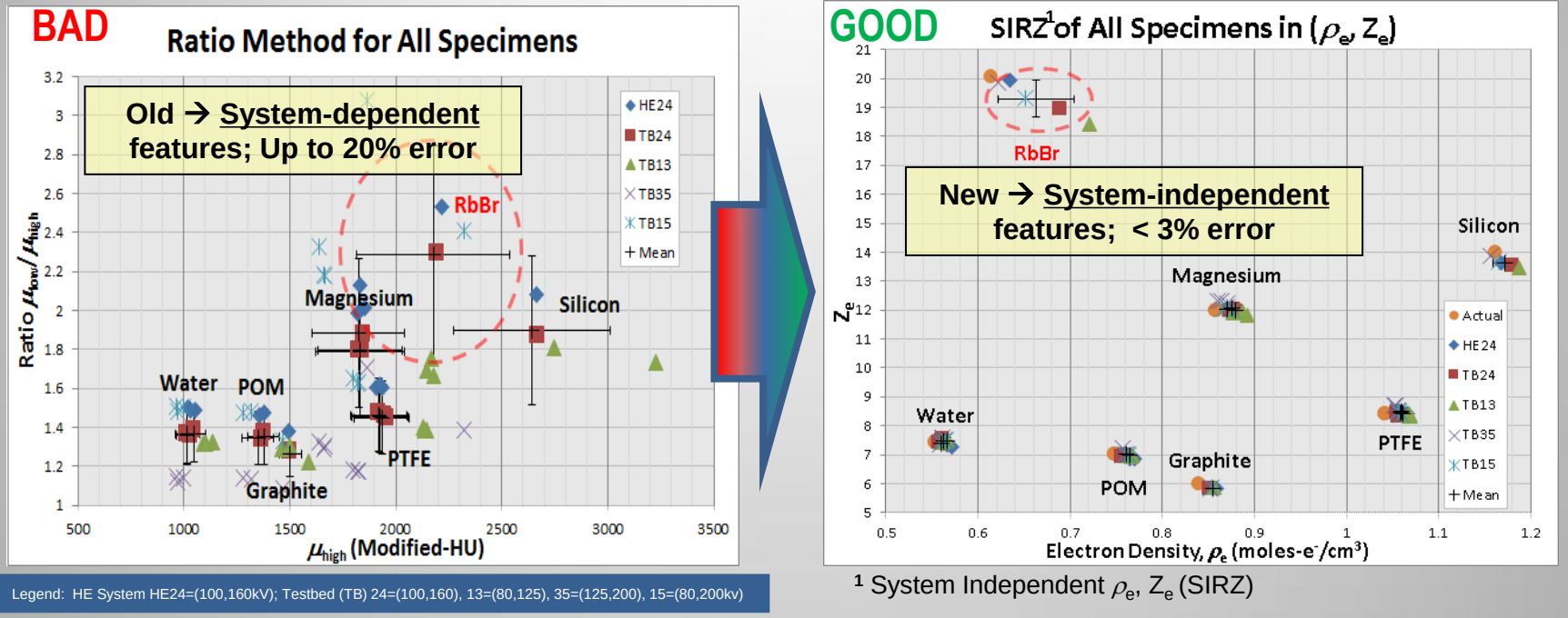

Legend: HE System HE24=(100,160kV); Testbed (TB) 24=(100,160), 13=(80,125), 35=(125,200), 15=(80,200kv)

[1] System Independent ρ_e, Z_e (SIRZ)

- **New X-ray features (ρ_e,Z_e) gave same results on two different MicroCT systems at LLNL; they are system-independent[2]**
  - Tested with 5 bare (homogeneous), 2 complex (heterogeneous) and 1 high-Z specimens
  - Used 2 different MicroCT scanners, 2 different detectors and 5 different spectra
  - No beam-hardening compensation (BHC) needed
  - Achieved <3% accuracy and <2% precision (req't ±3%) across all system variations (vs ±20% with current method) without RbBr
- **Future Work**
  - Automate and employ (ρ_e,Z_e) features for dual-energy CT systems at LLNL
  - Show that (ρ_e,Z_e) feature space
    - Can translate across different labs' MicroCTs and to other CT systems
    - Is backward compatible; i.e., we can use the data already acquired
  - Replace (μ_H, μ_L / μ_H) features with (ρ_e,Z_e)

[2] Azevedo, S. G., System-Independent Dual-energy Computed Tomography for Characterization of Materials, IEEE TRANSACTIONS ON NUCLEAR SCIENCE, VOL. *, NO. *, MONTH 2015

Back up slides

Precision Results – Standard Deviation as a % of Mean

- Plot shows ratio of standard deviation of mean values divided by mean value.
  - Composite material segmentations are denoted by (#-P), where "#" is the material of the container.
  - Low- and high-energy attenuation values (μ_L, μ_H) are computed using beam hardening compensation based on water.
  - Z_e, ρ_e show much lower variation (<2%, <1%) than μ_L (<20%) or μ_H (<14%).

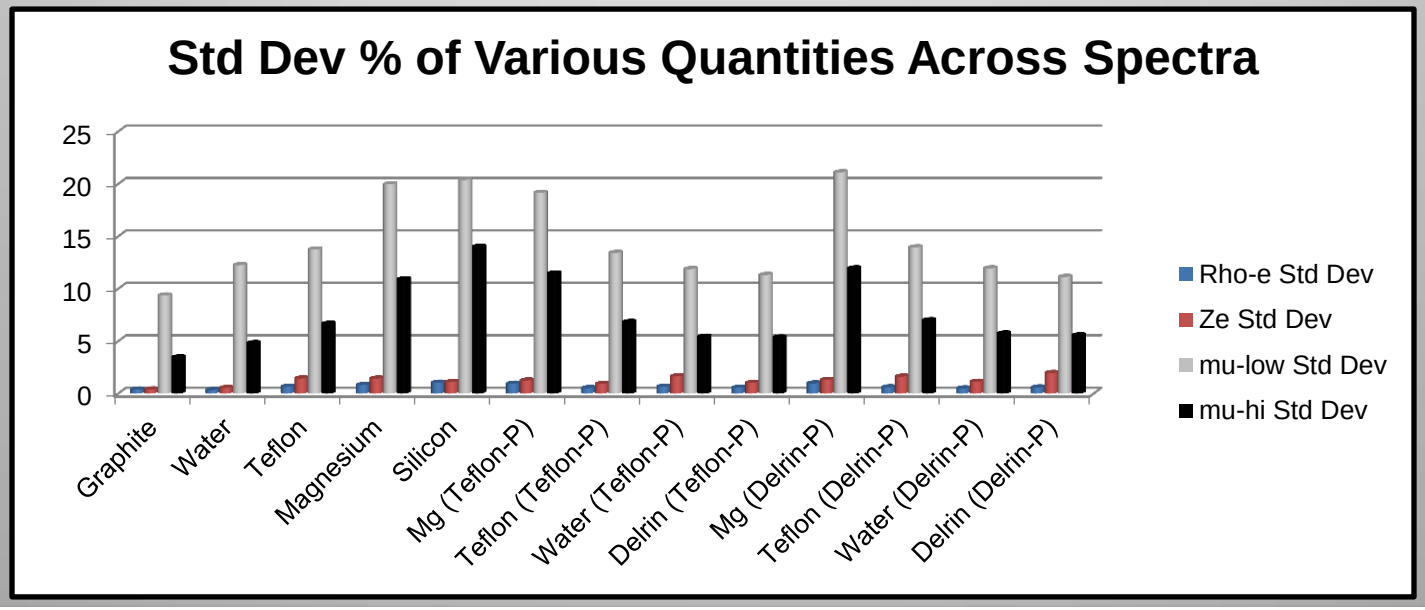

The PCD and DD methods produce similar results

OLD

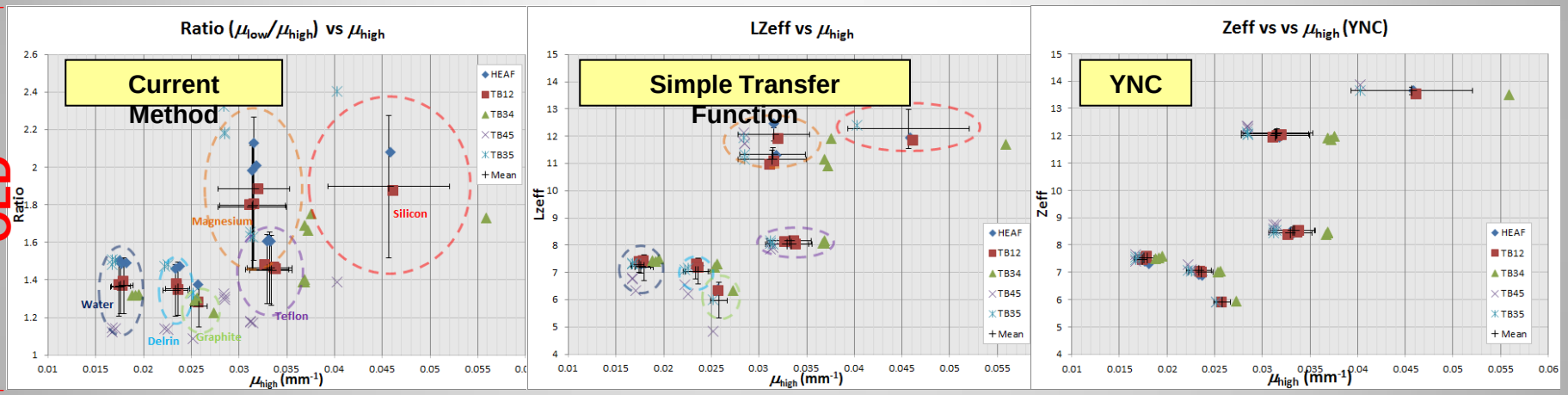

NEW (Proposed)

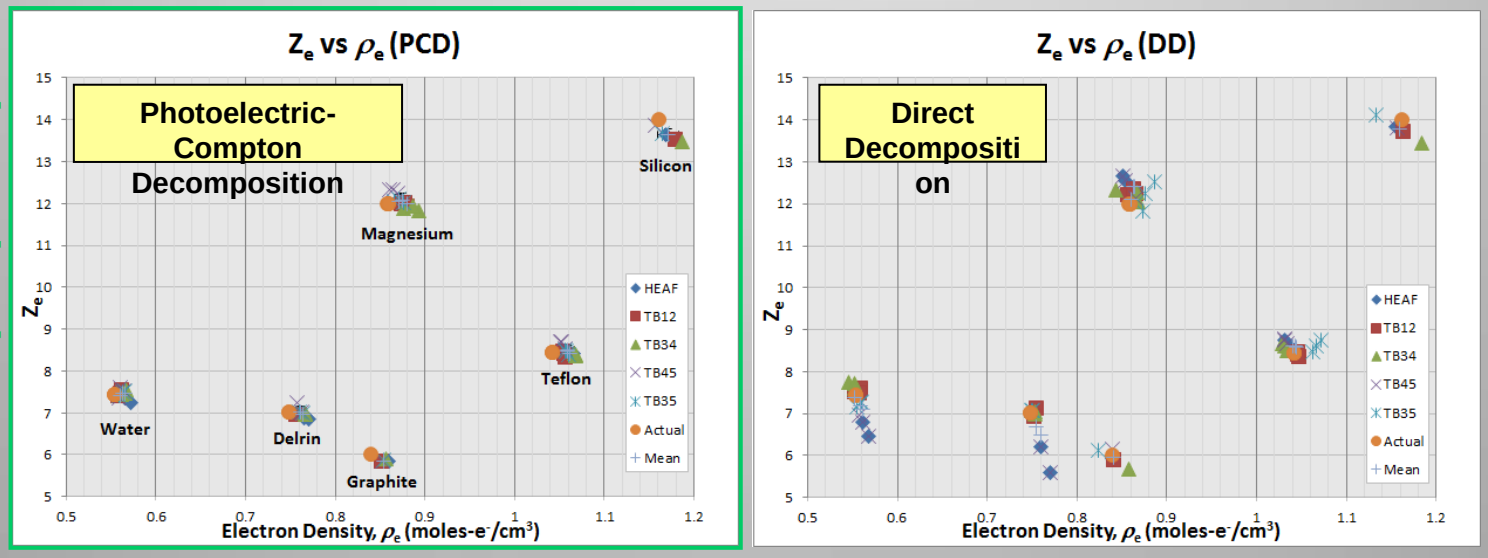

Legend: HEAF=(100,160kV); Testbed (TB) 12=(100,160), 34=(80,125), 45=(125,200), 35=(80,200kv). . "Actual" is physically measured density and elemental composition.

Summary of Photoelectric-Compton Decomposition

- Alvarez & Macovsky (1976)
  - Decomposition uses photoelectric and Compton contributions (Ac and Ap) to specify attenuation characteristics
  - Introduced the notion that full attenuation characteristics at every energy can be represented using a set of energy-independent values
    - Do not need to scan over a broad range of energy values; only in the energy range of interest in order to characterize a material.
    - Takes advantage of this fact by performing multiple scans at different energies over the applicable range, and using the results to validate the system.
  - Plots are in Ac, Ap signal space
- Ying, Naidu, Crawford (2006)
  - Proposed optimization technique using isotransmission curve intersections
  - Proposed scatter, streak and spectral corrections for EDS machines
  - Plots are in the Zeff vs high-energy attenuation (μ_H) signal space
- LLNL's Photoelectric-Compton Decomposition
  - Propose calibration of the system to known reference standards
  - Propose plot of Ze vs ρ_e to more closely follow material X-ray properties for a gain in both accuracy and precision

Overview

- **Overview**
  - **Describe analysis methods**
  - **Experimental plan**
  - **Reference materials and specimens**
  - **Experimental results**

Concerns with Current LLNL Techniques (1)

- It has been shown that $^{L}Z_{eff}$ calculations are sensitive to material density
- This definition of effective Z has inherent problems when attempting to accurately characterize HMEs:
  - Any selection of p does not fit all compounds equally well
  - The current value, p = 3.8**, is tuned to match the dependence of Z on photoelectric effects, and deviates when attenuation is dominated by Compton scattering
  - Calculated Z_{eff} is an ambiguous indicator of x-ray absorption
    - It has been demonstrated that elemental fractions can be tuned to yield multiple different compositions with the same computed Z_{eff}, and with different x-ray absorption properties
    - This in turn means that x-ray absorption properties cannot be reverse engineered from Z_{eff} values because they are nonunique

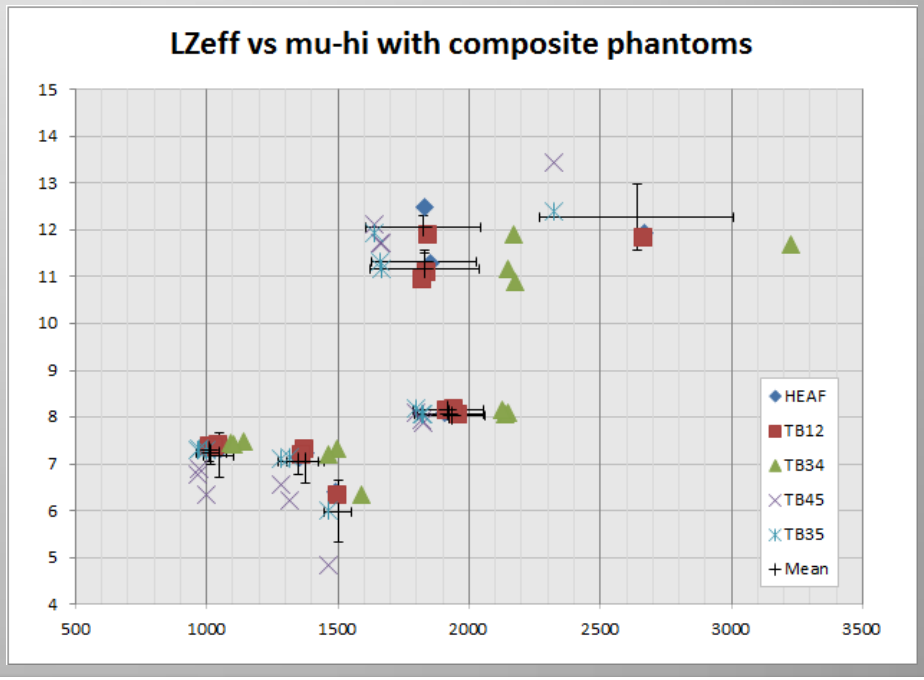

***TSL determined we should use p = 3.8*

Current Methods: Simple Transfer Function

- Current LLNL processing techniques make use of Z_{eff}, defined as:
  - The a's represent electron fractions contributed by constituent elements, and p is a constant tuned to approximate observed behavior. At the direction of TSL/DHS, we use p = 3.8
- Low- and high-energy measured attenuation values for known reference materials are combined with nominal Z_{eff} values to yield quadratic fit lines between Z_{eff} and attenuation ratio.
- Reference materials are separated into lower and higher Z groups.
- The lower group is used for a quadratic fit, while the upper group uses a constrained quadratic fit to generate a continuous curve.
- The specimen attenuation ratio is entered into the curve equation to yield a $^{L}Z_{eff}$ value, which is plotted against the high-energy attenuation value, in LMHU (where values are normalized such that water at high energy has mean value 1000).

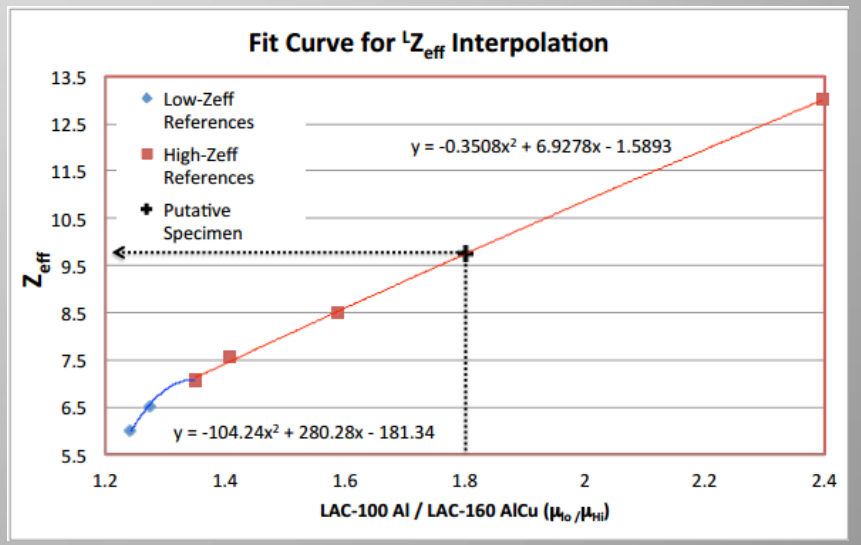

Concerns with Current LLNL Techniques (2)

- Since ${}^{L}Z_{eff}$ is tied directly to μ_L/μ_H, we have to deal with beam hardening correction
  - Beam hardening with a basis material that is close in attenuation to the specimen is required at low energy
    - Lack of beam hardening causes underestimation of attenuation value
    - Lack of or incorrect beam hardening causes changes in attenuation with specimen diameter
      - Underestimation (cupping) if the beam hardening material is much lower in Z
      - Overestimation (doming) if the beam hardening material is much higher in Z

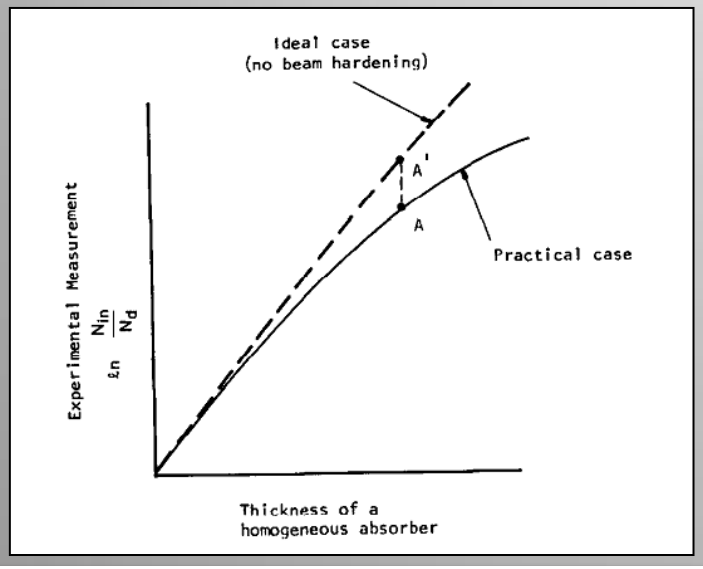

- Beam hardening effect resulting from polychromaticity of x-ray source spectra in a homogeneous absorber.
- Compensation is performed using extrapolation to a straight line from a polynomial fit to observed attenuation values.
  - Coefficients are determined using a basis material (at LLNL, water and aluminum have been used).

Image Source:
A. Kak, M. Slaney, Principles of Computerized Tomographic Imaging, Society for Industrial and Applied Mathematics, Philadelphia, PA, 2001.

BHC Artifacts

100kV Al Filtered Reconstructions

Low-Z Material

High-Z Material

No Beam Hardening Compensation

H_2O BHC

Al BHC

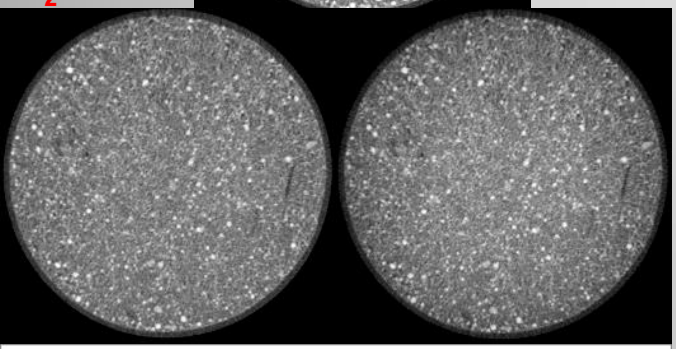

H_2O BHC

Al BHC

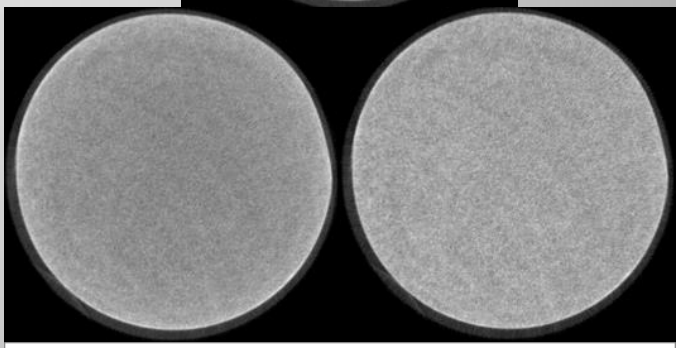

Doming effects			
160kV	1080		
	Al BHC	H2O BHC	No BHC
100kV	1599	1611	1564
Ratio	1.481	1.492	1.448

Cupping effects			
160kV	1481		
	Al BHC	H2O BHC	No BHC
100kV	3614	3227	2992
Ratio	2.441	2.180	2.021

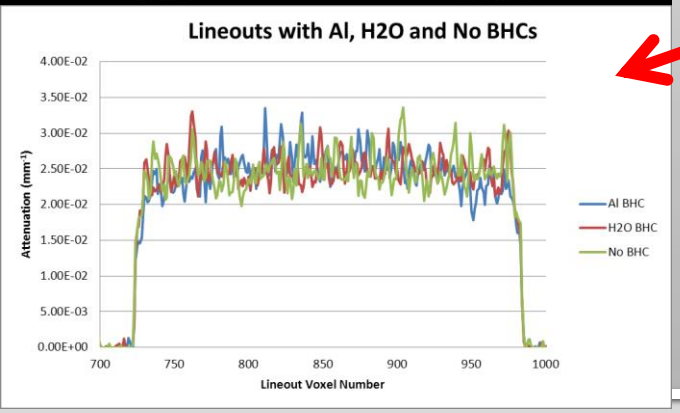

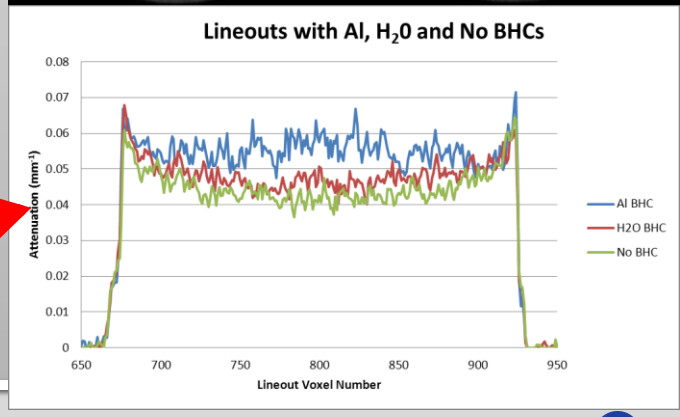

Moving Forward

- Summary of issues:
  - Require method that allows comparison between machines
  - High- and low-energy channel response can vary between machines – any method based on manipulation of μ_L, μ_H will see variation across machines
  - Zeff is more effective than using projection values alone, but is still limited due to a disconnect with physical properties of materials
  - Beam hardening is not universally applicable across a wide range of specimen Z values

- Proposed solutions:
  - Move to a system that represents materials using Z_e, to more closely track with material x-ray properties
  - Move to dual (or multiple) energy decomposition to remove the need for beam hardening compensation

How do we compute Ze, ρ_e?

- Two proposed methods
  - Direct Decomposition
    - Developed at LLNL
  - Photoelectric-Compton Decomposition
    - Discussed by Alvarez & Macovsky
    - Extended by Ying, Naidu, Crawford
    - Extended at LLNL

Direct Decomposition from Transmissions to (Z_e, ρ_e)

1. **For each projected ray through the object:**
   1. **Measure the Transmissions (Ti) for N ≥ 2 spectra;**
   2. **Find the values {Ze, Me} that provide the minimum error:**

$$\sum_i^N \left(\int dE_x S_i[E_x] Exp[-\sigma(Z_e, E_x) M_e] - T_i \right)^2$$

x: is the path through the object

S_i: are the spectral responses (normalized to 1.0)

E_x: is the x-ray energy

$\sigma(Ze, E_x)$: is the x-ray cross section per mole of electrons

M_e: is the areal electron density

Z_e: is the effective atomic number

2. **Backproject the M_e to get an image of the electron density img_R** ρ_e : ➔
3. **Backproject an image img_{mz} from $M_e(Z_e)^p$** (p ~ 3.0)
4. **Convert this to an image of Z_e :** $$img_{Ze} = (img_{mz}/img_R)^{1/p}$$

Photoelectric-Compton Decomposition

- Attenuation generally follows the Beer-Lambert Law:

$$I = I_o e^{-\mu l}$$

- Projections (P) are obtained using the formula:

$$P = -\ln \frac{I}{I_0} = \mu l$$

- The attenuation (μl) can be decomposed into photoelectric and Compton contributions, as a function of energy:

$$Atten(E) = \int \mu(x,y,z,E)dl = f_{KN}(E)\int a_c dl + f_p(E)\int a_p dl = -f_{KN}(E)A_c - f_p(E)A_p$$

- Integrating over the spectral energy density (*S*), the above mono-energetic equations can be extended to poly-energetic systems. Using 2 different spectra, this becomes a problem of solving a system of 2 equations with 2 unknowns (A_c, A_p).

$$P_L = -\ln\left[\int S_L(E)exp\left[-f_{KN}(E)A_c - f_p(E)A_p\right]dE\right] + \ln\int S_L(E)dE \qquad \text{(Low energy projection)}$$

$$P_H = -\ln\left[\int S_H(E)exp\left[-f_{KN}(E)A_c - f_p(E)A_p\right]dE\right] + \ln\int S_H(E)dE \qquad \text{(High energy projection)}$$

I $\qquad$ I_0

Important: Spectra must be well known, and images must be well registered!

Z. Ying, R. Naidu, C. R. Crawford, *Dual Energy Computed Tomography for Explosive Detection*, Journal of X-Ray Science and Technology, 2006, no. 14, pp. 235-256.

Recommendations Going Forward

- Photoelectric-Compton Decomposition recommended for processing of LLNL data going forward
  - Shows tighter results on R&D experimental data than current LLNL techniques when viewing data in the Z_e, ρ_e feature space.
  - Direct decomposition is still under development, with possible extension through:
    - Calibration techniques (to known references)
    - Multiple (>2) spectrum analysis.

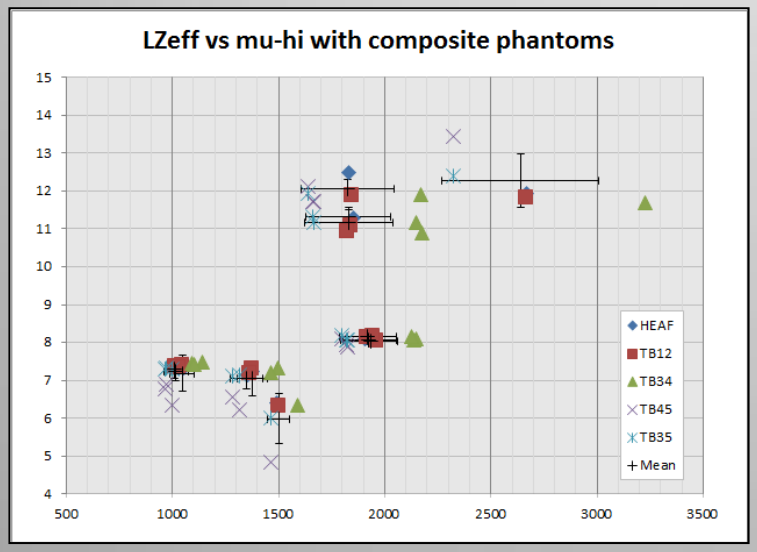

Simple Transfer Function (current LLNL method)

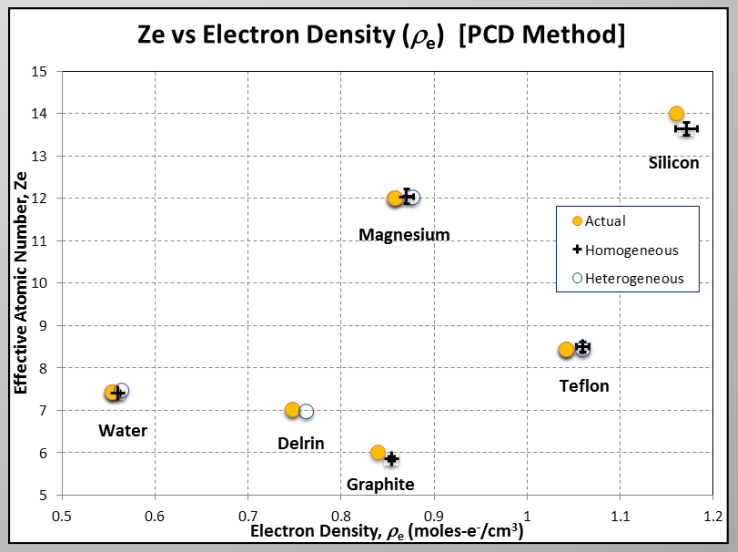

Photoelectric-Compton Decomposition (recommended)

Changes to Data Processing (Current)

Current:

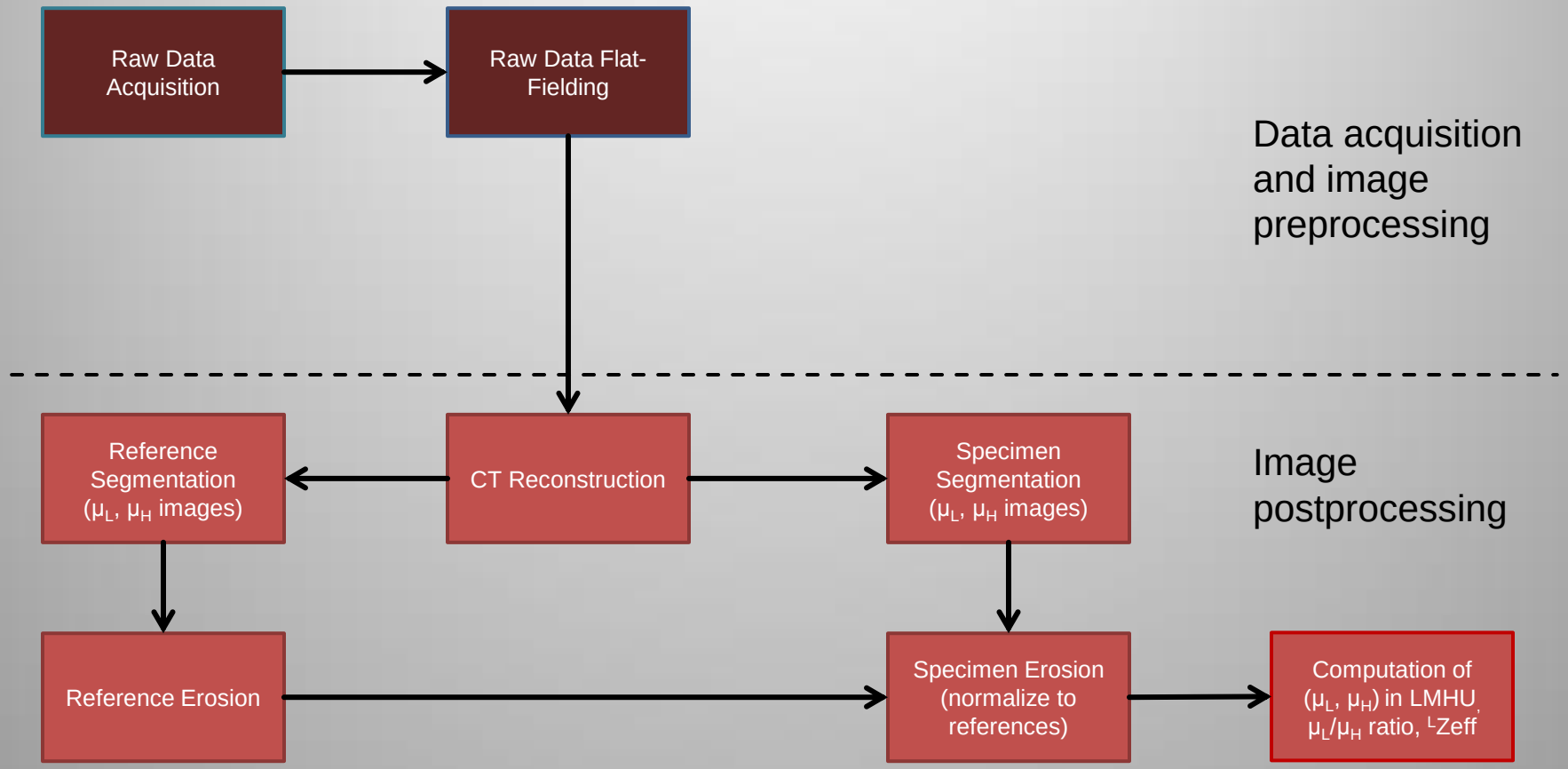

Changes to Data Processing (Proposed)

Proposed:

- Data flow for photoelectric-Compton decomposition (new operations and procedures in green):

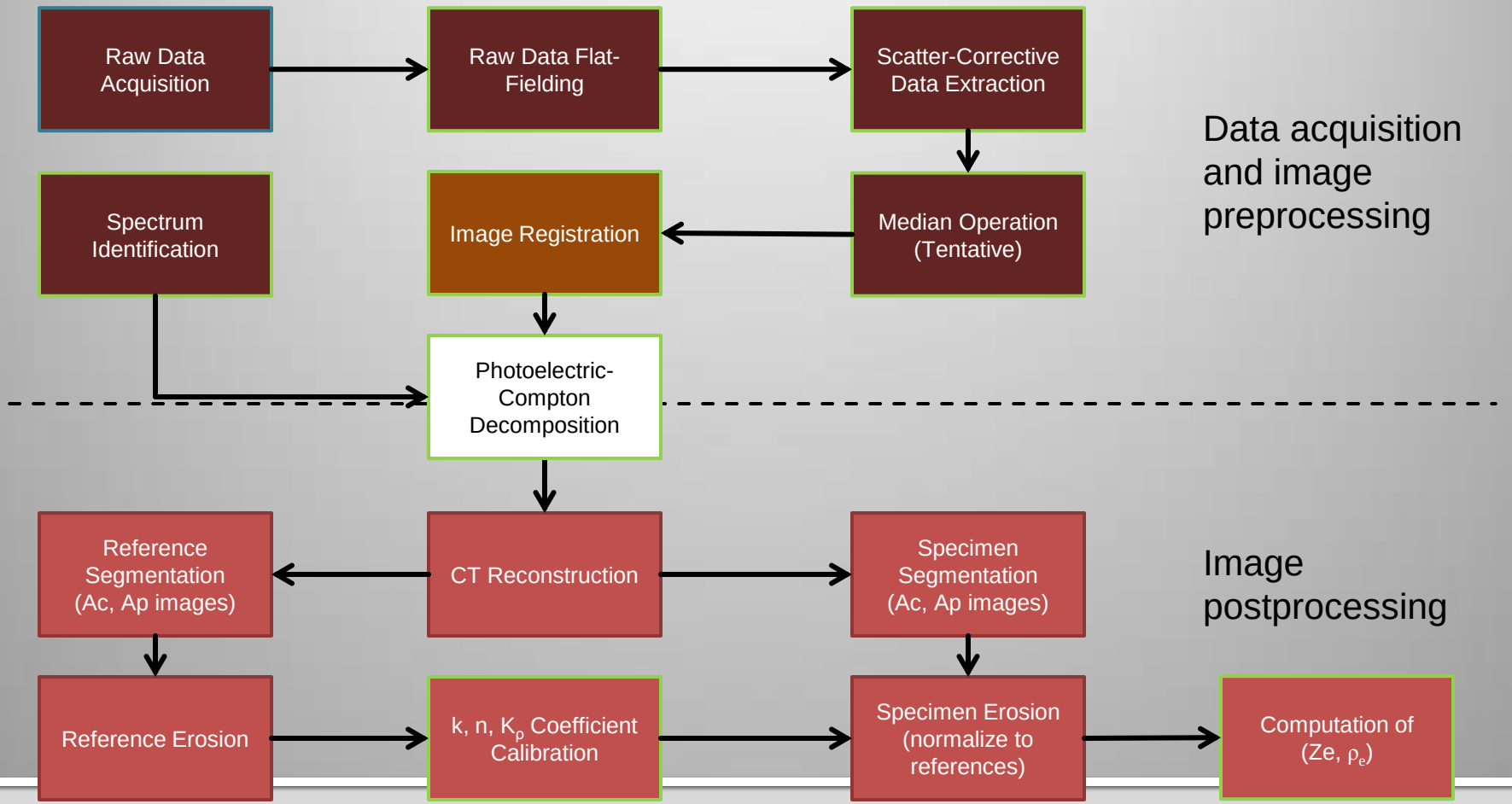

Flatfielding Radiographs from Raw-images

- **Raw Radiographs require individual-pixel corrections for dark-current and relative gain.**
- **Three files are used:**
  1. **drk** (x-ray source off: image includes dark current and offset)
  2. **lit** (Full imaging intensity ~95% of detector range)
  3. **mid** (x-ray source is set to 2/3 of Lit)

A. **drk image is subtracted from mid and light**

M = mid – drk ; L = lit – drk ;

B. **Medians of imgM and imgL are M_{med} and L_{med} respectively**

C. **Gain coefficients for each pixel (coordinates { I, j }) are determined separately for the exposure segments above and below M_{med}:**
   A. $GM_{ij} = M_{med} / imgM_{ij}$
   B. $GL_{ij} = (L_{med} - M_{med}) / (L_{ij} - M_{ij})$

D. **To convert a raw (raw) image to a radiograph (rad)**
   A. $rad_{ij} = GM_{ij} (raw_{ij} - drk_{ij})$
   B. If $raw_{ij} > M_{med}$; $rad_{ij} \rightarrow M_{med} + GL_{ij} (raw_{ij} - M_{ij})$

E. **NOTE: if $rad_{ij} < 0$, values are <u>not</u> clipped.**

Removing Scatter and Detector Blur from Transmission Measurements

An image segment from a radiograph shows the x-ray transmission through three 1/2-inch rods as seen through a slit collimator

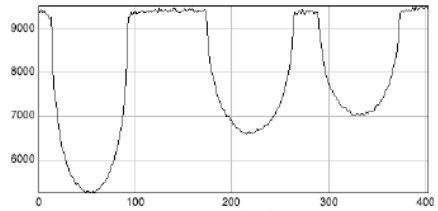

The transmission lineout a—a shows the image intensity along the slit

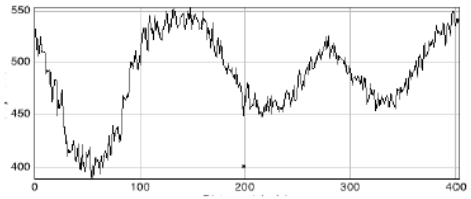

Lineout b—b shows blur from the "in-slit" radiation spreads across the image and into the un-radiated area of the detector.

As seen at right in lineout c—c, there is a component of blur (d—d) underlying the image. This blur has a different spectral dependence than the scintillator. It must be removed to obtain accurate x-ray intensity measurement.

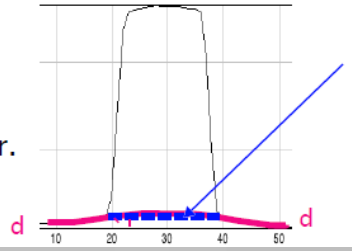

A "pedestal is subtracted from the in-slit intensity to correct for blur and scatter. This amplitude of this pedestal varies along the slit as shown in the lineout b—b.

We subtract the blue dotted line as a linear approximation of scatter and blur contributions (pink). Seven rows are extracted and median-filtered to a single row. Edge blur within this row is Fourier deconvolved using an MCNP-calculated blur function.

Removing Scatter and Detector Blur from Transmission Measurements

- Scatter and blur can have significant effects if not addressed

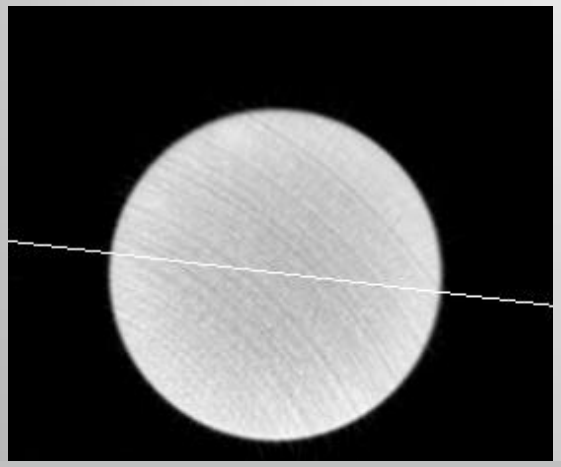

1” cylindrical silicon reference specimen

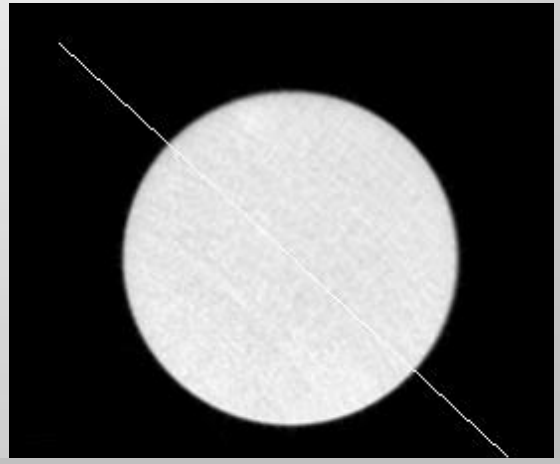

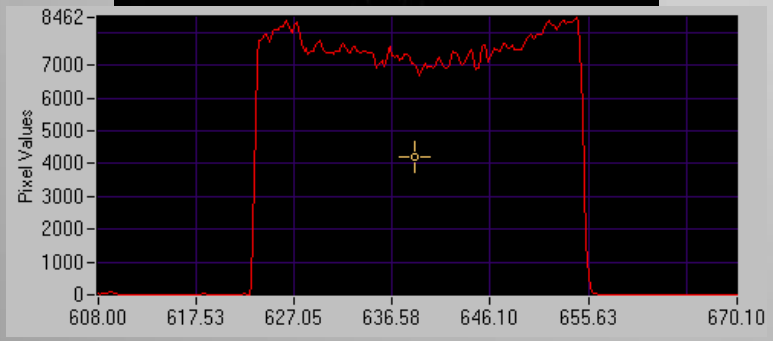

No scatter/blur correction

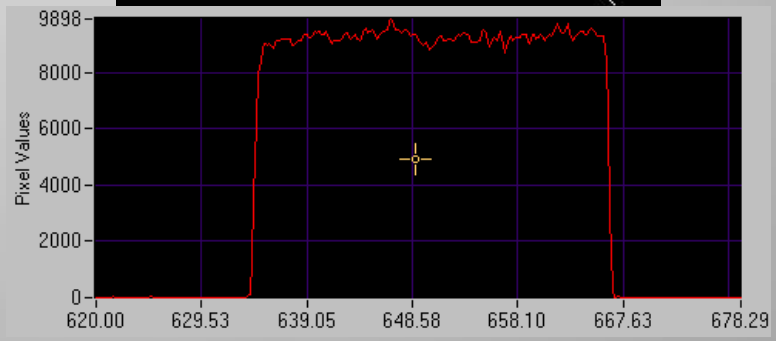

Scatter/blur correction applied

Median Filtering

- Median filtering
  - Primarily used during R&D on homogeneous samples to reduce data processing time.
  - Blurs data along the slice plane direction (across detector rows)

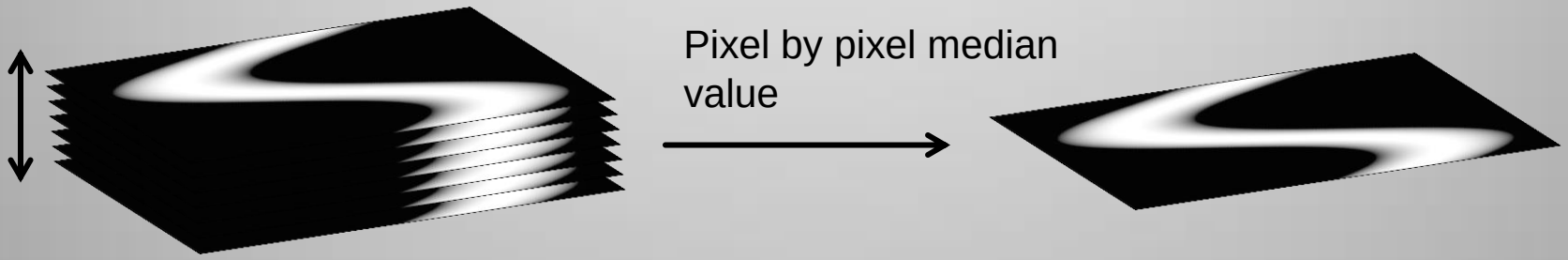

7 sinograms from 7 detector rows

Resulting sinogram

**This step will most likely not occur during production, as production data analysis must be material homogeneity-independent.*

X-ray Response Models for Direct- and Photo/Compton-Decomposition

- **X-ray Source Spectra** are calculated using validated published models.
  - Tungsten Target, 11-degree Takeoff angle, 5-mm Be internal filtration.
- **X-ray Filtration**: based on measured properties if accurately known. Otherwise filter thicknesses adjusted to match measured attenuation.
- **Scintillator Response** and **Detector Blur** are taken from MCNP calculations by Morry Aufderheide.
  - Amorphous Silicon areal detector arrays from Thales and Perkin Elmer (PE)

Spectrum	1*	1A	2*	2A	3	4	5
Source kV	100	100	160	160	80	125	200
Al filter (mm)	1.943	1.25	1.943	1.25	0.5		
Cu filter (mm)		0.07	1.905	2.105	0.14	1.1	3.0
Detector	Thales	PE	Thales	PE	PE	PE	PE

*For this R&D effort, source filters for the Thales panel were well known, whereas for the Perkin Elmer source filters are approximate.

Finkelshtein: A. L. Finkelshtein and T. O. Pavlova, *Calculation of X-Ray Tube Spectral Distributions*, X-Ray Spectrom. 28, (1999).
SpekCalc_1: G.G Poludniowski, Evans PM., *Calculation of x-ray spectra emerging from an x-ray tube. Part I. electron penetration characteristics in x-ray targets*, Med Phys., June 2007, 34(6), pp. 2164-74.
SpekCalc_2: G.G Poludniowski, *Calculation of x-ray spectra emerging from an x-ray tube. Part II. X-ray production and filtration in x-ray targets*, Med Phys., June , 34(6), pp. 2175-86.

Examples of Spectral Responses and Fits to Attenuation Data on Cylindrical Specimens

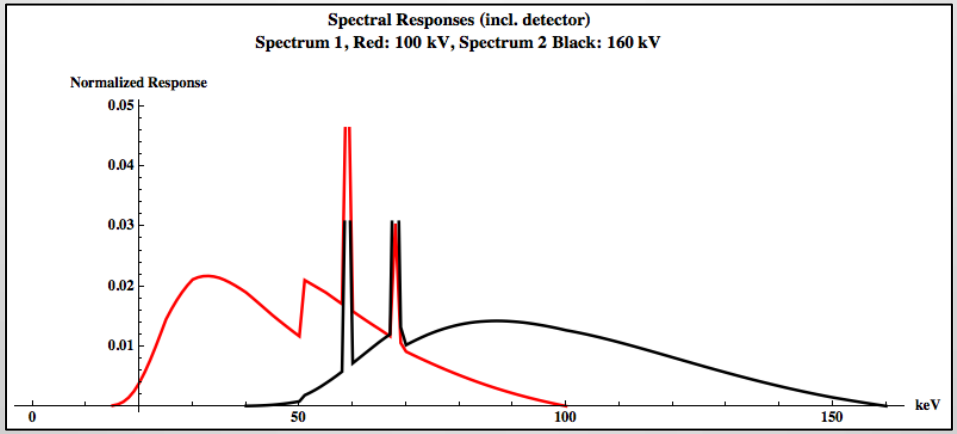

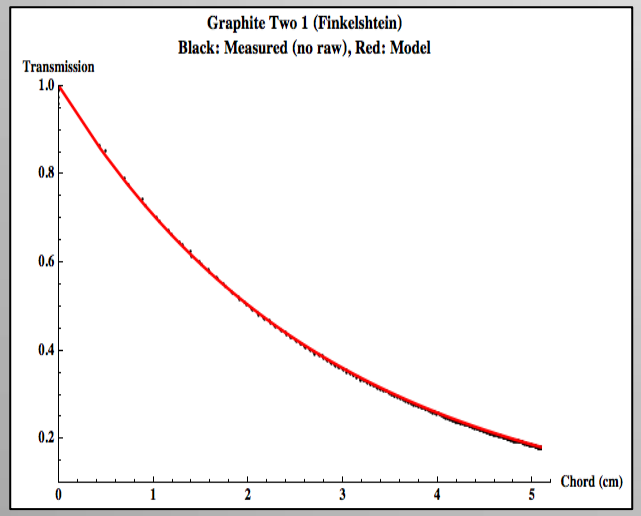

Spectrum 1: calculated vs measured transmission through a 2-inch diameter graphite cylinder

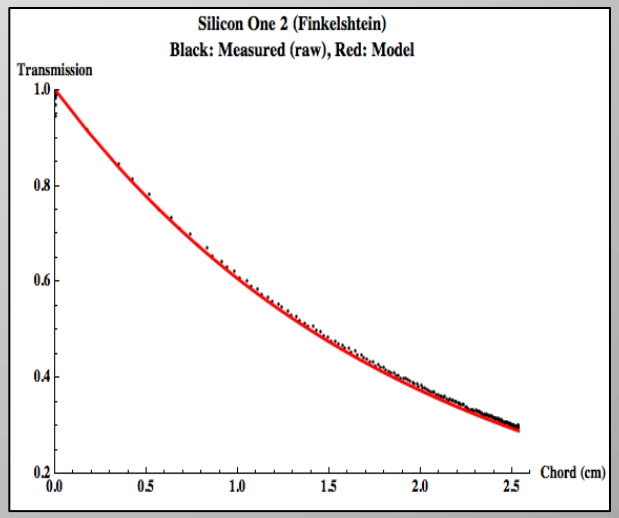

Spectrum 2: calculated vs measured transmission through a 1-inch diameter silicon cylinder

Reference Normalization for Z_e

- Measured effective atomic number (Z_e) is computed using the formula:

$$Z_e = k\left({}^{a_p}/_{a_c}\right)^{1/n}$$

- *k, n* are constants
- Values for *k, n* are calculated using photoelectric and Compton coefficient values extracted from the known Reference Standards imaged in the lower slit of the experiment.
  - Reference standards are reference material samples in which we have a high confidence in composition and physical properties.
  - Nominal values are provided using the program ZeCalc (LLNL).
  - A minimum mean square error (MMSE) fit is performed.

Material	Nominal Ze
Graphite	6
Delrin	7.01
Water	7.43
Teflon	8.44
Magnesium	12
Silicon	14

Reference Normalization for Electron Density

- Measured electron density is approximated using the formula:

$$\rho_e = K_\rho a_c$$

- is a computed constant
- Values for are calculated using Compton coefficient values extracted from the known Reference Standards imaged in the lower slit of the experiment.
  - Reference standards are reference material samples in which we have a high confidence in composition and physical properties.
  - Nominal values are computed using data obtained from material assay and from provided datasheets on material purity and composition.
  - A linear least squares fit is performed.

Material	N
Graphite	0.901
Delrin	0.748
Water	0.554
Teflon	1.044
Magnesium	0.857
Silicon	1.162

Experimental Plan: Introduction

- Test Plan 75 – Multi-Energy Decomposition
  - Focuses on using known materials as references and specimens to establish a baseline on performance of dual energy decomposition techniques
  - Two systems and multiple spectra were used in order to demonstrate independence of measured values from system response
  - New carousel of assayed materials was used to guarantee desired accuracy
  - Simulations performed to validate experimental results

Results – PCD Coefficient Stability

- k, n coefficients from PCD examined from TP75 data processed using the 5 mentioned spectral pairs over 7 specimens
- Empirically derived k, n values were used to extrapolate Z values vs photoelectric/Compton ratio values across a broad range.
- Upper end standard deviation of 0.072 in Z (typical Z scanned is on the order of 6-15)

→ k, n values observed in TP75 data

were very stable across spectral pairs!

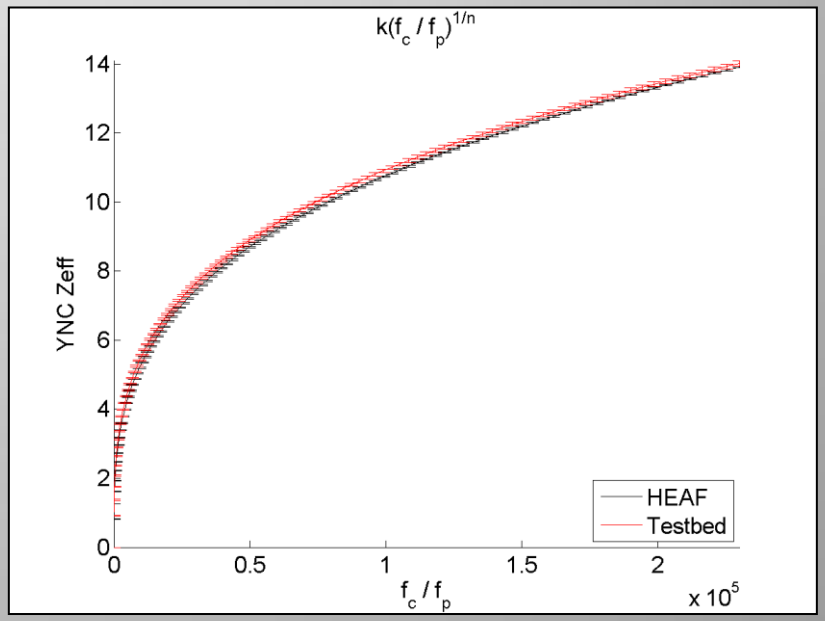

Summary

- Two different systems with identifiably different high- and low- energy characteristics were used.
- Results obtained using dual-energy decomposition techniques are significantly tighter (<3%) than those obtained using standard LLNL techniques (>20%) reliant on high and low energy projection values.
- Presenting results in (Z_e, ρ_e) space produces tighter clustering of materials of identical composition than projection value-based techniques.

Recommendations and Future Work

Recommendations:

- Change to a Z_e, ρ_e feature space for the analysis of new data
- Use LLNL's PCD for the analysis of new data.

Future work:

- Validation of changes to PCD processing (image flat-fielding, scatter correction, spectrum identification, median filter and Z_e calculation)
- Development of image registration tools
- Development of automated PCD software
- Validation of PCD's backward compatibility

- Extension of LLNL Direct Decomposition to multiple spectrum analysis
- Extension of LLNL Direct Decomposition to include normalization to references

Colors and arrows

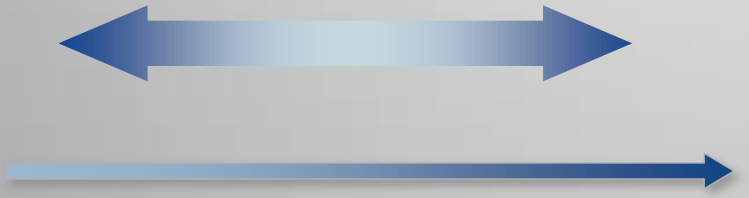

Summary box is now full width bleed